Observation of Soot Superaggregates with a Fractal Dimension of 2.6 in Laminar Acetylene/Air Diffusion Flames

Christopher M. Sorensen,* Wongyo Kim, Dan Fry, Dan Shi, and Amitabha Chakrabarti

Department of Physics, Kansas State University, Manhattan, Kansas 66506-2601

Received January 14, 2003. In Final Form: April 11, 2003

We report the observation of a novel phase of soot in an acetylene/air laminar diffusion flame. As was measured by a small-angle light scattering apparatus, the phase consists of about 10-μm superaggregates with a fractal dimension of $D \simeq 2.6$. This phase coexists with submicrometer $D \simeq 1.8$ soot fractal aggregates typical for most flames. Both percolation and shear-induced restructuring are considered as possible mechanisms of formation for those superaggregates.

I. Introduction

It is now well established that carbonaceous soot in flames grows, after an initial period of nucleation and surface growth, via the process of diffusion-limited cluster aggregation (DLCA) to form fractal aggregates with a fractal dimension of $D \simeq 1.8$.[1−5] These aggregates are composed of roughly spherical monomers with a diameter of 30−60 nm that form during the initial period. The aggregates are usually submicrometer, although examples of supermicrometer aggregates have been reported.[6]

Recently, we have observed two aspects of soot morphology in acetylene/air diffusion flames that suggest the simple picture that $D \simeq 1.8$, DLCA aggregates does not hold true in the supramicrometer range. First, in situ optical photography evidence was given for an aerogelation process in these flames.[7] At that time, static light scattering (SLS) measurements indicated submicrometer $D \simeq 1.8$ aggregates and strongly implied a second phase of soot involving aggregates larger than 5 μm. Unfortunately, this second phase could not be quantitatively described because our light scattering apparatus was limited to angles greater than about 1° and, hence, the detection of sizes less than 5 μm.

In a second work involving acetylene/air diffusion flames, Sorensen and Hageman[8] showed that the soot in the size range of $25 \leq R_g \leq 120$ μm, where R_g is the aggregate radius of gyration, was flat, that is, quasi-two-dimensional, and had a fractal dimension of $D \simeq 1.4$. This fractal dimension and the two-dimensional shape are consistent with a picture wherein supramicrometer soot clusters confined to the two-dimensional annular flame front aggregate via a two-dimensional DLCA process.

Here, we return again to this fascinating, heavily sooting acetylene/air diffusion flame, but now we are armed with a new piece of apparatus that allows us to quantitatively measure light scattered to angles as small as 0.05°, which is equivalent to length scales as large as 100 μm. Thus, we extend the SLS measurement in our first paper. We find supramicrometer aggregates with a fractal dimension of $D \simeq 2.6$. We know of no previous reports of such aggregates in the combustion literature. The formation mechanism for these aggregates is not yet known. However, we will propose two likely scenarios: (1) percolation of smaller $D \simeq 1.8$ aggregates into percolated superaggregates with $D \simeq 2.6$ and (2) restructuring of large $D \simeq 1.8$ aggregates to form more compact structures.

II. Experimental Method

The experiment involved a heavily sooting acetylene/air diffusion flame. The flame was essentially the same as that used previously.[7,8] It was produced on a simple diffusion burner composed of a 0.9-cm i.d. brass tube through which acetylene or mixtures of acetylene and methane could be passed at a variable flow rate. The flame that was ignited above this tube burned in the ambient air with various screen buffers to stabilize the flow. The flame was bright yellow-white at its base but cooled with increasing height above the burner, h, to dull orange and then black and narrow laminar flowing soot aerosol by $h \simeq 8$ cm, depending somewhat on the flow rate. Light scattering data where taken as a function of the height above the burner, a height of $h = 15$ cm corresponding to a time of about 100 ms when the acetylene flow rate was 6.6 cm^3/s.

SLS was used to measure the structure of the soot aggregates in the flame.[9] These measurements gave the scattered intensity $I(q)$ as a function of q, the scattering wave vector

$$q = 4\pi\lambda^{-1} \sin(\theta/2) \quad (1)$$

In eq 1, λ is the optical wavelength and θ is the scattering angle. An argon ion laser operating at $\lambda = 488$ nm was used as the light source. Two different devices measured $I(q)$. The primary apparatus was a small-angle light scattering device designed

* Corresponding author. E-mail: sor@phys.ksu.edu.

(1) Sampson, R. J.; Mulholland, G. W.; Gentry, J. W. Structural Analysis of Soot Aggregates. *Langmuir* **1987**, *3*, 272−281.

(2) Zhang, H. X.; Sorensen, C. M.; Ramer, E. R.; Olivier, B. J.; Merklin, J. F. In Situ Optical Structure Factor Measurements of an Aggregating Soot Aerosol. *Langmuir* **1988**, *4*, 867−871.

(3) Megaridis, C. M.; Dobbins, D. A. Morphological Description of Flame-Generated Materials. *Combust. Sci. Technol.* **1990**, *71*, 95−109.

(4) Sorensen, C. M.; Cai, J.; Lu, N. Light-Scattering Measurements of Monomer Size, Monomers Per Aggregate, and Fractal Dimension for Soot Aggregates in Flames. *Appl. Opt.* **1992**, *31*, 6547−6557.

(5) Köylü, U. O.; Faeth, G. M. Structure of Overfire Soot in Buoyant Turbulent Diffusion Flames at Long Residence Times. *Combust. Flame* **1992**, *89*, 140−156.

(6) Sorensen, C. M.; Feke, G. D. The Morphology of Macroscopic Soot. *Aerosol Sci. Technol.* **1996**, *25*, 328−337.

(7) Sorensen, C. M.; Hageman, W. B.; Rush, T.; Huang, H.; Oh, C. Aerogelation in a Flame Soot Aerosol. *Phys. Rev. Lett.* **1998**, *80*, 1782−1785.

(8) Sorensen, C. M.; Hageman, W. B. Two-Dimensional Soot. *Langmuir* **2001**, *17*, 5431−5435.

(9) Sorensen, C. M. Light Scattering from Fractal Aggregates: A Review. *Aerosol Sci. Technol.* **2001**, *35*, 648−687.

10.1021/la034063h CCC: $25.00
Published on Web 07/31/2003

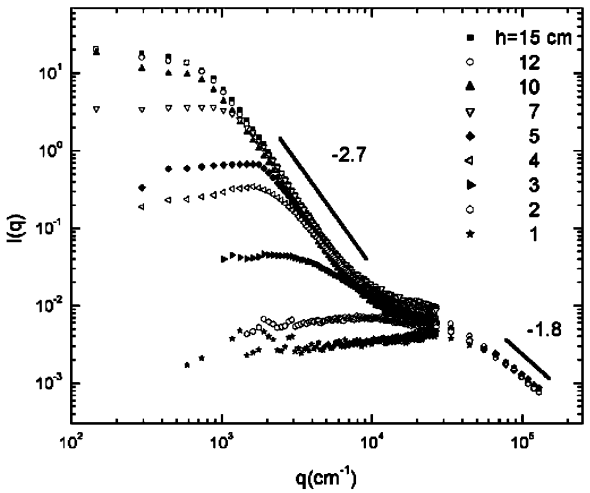

Figure 1. Scattered light intensity as a function of the wave vector for an acetylene/air diffusion flame with a flow rate of 6.6 cm^3/s at different heights above the burner, h.

after Ferri[10] that allowed q values in the range $100 \leq q \leq 3 \times 10^4$ cm^{-1}. For large values of q, we used a moveable photomultiplier that could detect light for the range $10^4 \leq q \leq 1.5 \times 10^5$ cm^{-1}.

One might also capture the soot for transmission electron microscopy (TEM) analysis. However, methods for the analysis of such large soot particles with fractal dimensions greater than 2.0 are not well developed. Thus, for now we only report the results of nonperturbative light scattering.

III. Results

The scattering results are shown in Figure 1. The primary variable is the height above burner orifice, h, which increases with increasing time for aggregation. At low heights, $h = 1$ and 2 cm, a result typical of numerous previous measurements of soot in flames is seen.[9] Namely, submicrometer (radius of gyration, $R_g \simeq 0.25$ μm) soot aggregates (the spherical monomers that form the aggregate have radii of $a \simeq 25$ nm, measured via TEM) with a fractal dimension of $D \simeq 1.8$. It is well established for flames that such aggregates are a result of DLCA in the dilute limit.

Unusual to these heavily sooting flames is the appearance, with increasing height, of a very strong second feature at lower q. The slope of this feature ranges from about -2.5 at $h = 4$ cm to -2.8 at $h = 15$ cm, and it bends over to a plateau at lower q implying sizes on the order of 5 μm at $h = 4$ cm to 25 μm at $h = 15$ cm. At $h = 15$ cm, the increase in the scattered intensity is a remarkable 3 orders of magnitude. We interpret this feature to indicate the onset of supramicrometer "superaggregates" with a fractal dimension of $D \simeq 2.6$. Other measurements with acetylene flames at different flow rates and with flames diluted with methane yield similar results. When the methane fraction is 75% or greater, the superaggregate phase does not appear.

Care must be taken with regard to the issue of whether the scattering $I(q)$ accurately represents the structure factor $S(q)$ of these large, dense superaggregates. It is now well established[9,11,12] for light scattering from soot aggregates that $I(q) \propto S(q)$ when $D < 2$. It can be shown that this proportionality holds because the effective phase shift parameter $\rho = 2kR_g f|m - 1|$, where $k = 2\pi/\lambda$, m is the refractive index of the aggregate material, and f is the volume fraction of primary particles in the aggregate, goes to 0 as $R_g \rightarrow \infty$.[9] This is the so-called Rayleigh–Debye–Gans regime. However, $\rho \rightarrow \infty$ as $R_g \rightarrow \infty$ when $D > 2$. Our results for the superaggregates imply $D \simeq 2.6$ with $R \simeq 10\,\mu$m. Then, with $m = 1.56 - i0.56$, a commonly accepted value for soot,[13] one obtains $\rho \simeq 70$. Thus, we cannot expect $I(q)$ to represent $S(q)$. However, in recent work[14] one of us has shown for spheres that when $\rho \gg 1$ the scattering results from only a thin layer with thickness R/ρ at the surface of the sphere. This is equivalent to $I(q)$ being proportional to the structure factor of an annular surface layer of the sphere. With this, we infer that the $I(q)$ we measure for the superaggregates reflects the structure of the surface of these aggregates. Thus, we measure the radius of the *surface* of the aggregates, which is the radius of the aggregate, and the aggregate *surface* fractal dimension. Note, however, that typically for aggregates the surface and mass fractal dimensions are equal. This is true for both DLCA aggregates and for percolation clusters[15] in all spatial dimensions. This latter fact is important for one of our formation scenarios to be described in the following.

IV. Discussion

The appearance of $D \simeq 2.6$ superaggregates in Figure 1 is dramatic with no values of D intermediate between the 1.8 value of the submicrometer soot and 2.6. Furthermore, despite the onset of the $D \simeq 2.6$ structure, the $D \simeq 1.8$ region remains for $q \geq 3 \times 10^4$ cm^{-1}, which corresponds to length scales smaller than 0.3 μm. Thus, the superaggregates are not simple fractals. Instead, they are heterogeneous with $D \simeq 1.8$ for length scales less than about 0.3 μm and $D \simeq 2.6$ for length scales greater than about 1 μm with some unknown crossover morphology in between.

We now propose two scenarios to explain the formation of these $D \simeq 2.6$ superaggregates of soot. The first scenario contends that these superaggregates form when the growing $D \simeq 1.8$, DLCA aggregates become large enough to fill the entire space. When this happens, the growth crosses over to a percolation process that is known to form $D \simeq 2.55$ aggregates in three dimensions.[16–18] The second scenario is less quantitative but relies on observations by others that large DLCA aggregates can restructure to denser aggregates when subjected to shear.

1. Percolation Scenario. The percolation scenario is supported by recent related work[19] in which we have performed three-dimensional, DLCA simulations in a cubical box. We use realistic monomer volume fractions as low as $f_v = 5 \times 10^{-4}$. The simulations begin by placing

(10) Ferri, F. Use of a Charge Coupled Device Camera for Low-Angle Elastic Light Scattering. *Rev. Sci. Instrum.* **1997**, *68*, 2265.

(11) Cai, J.; Lu, N.; Sorensen, C. M. Comparison of Size and Morphology of Soot Aggregates as Determined by Light Scattering and Electron Microscope Analysis. **1993**, *9*, 2861–2868.

(12) Farias, T. L.; Koylu, U. O.; Carvalho, M. G. Range of Validity of the Rayleigh-Debye-Gans Theory for Optics of Fractal Aggregates. *Appl. Opt.* **1996**, *35*, 6560–6567.

(13) Dalzell, W. H.; Sarofim, A. F. Optical Constants of Soot and their Application to Heat-Flux Calculations. *J. Heat Transfer* **1987**, *9*, 100–104.

(14) Sorensen, C. M.; Fischbach, D. J. Patterns in Mie Scattering. *Opt. Commun.* **2000**, *173*, 145–153.

(15) Strenski, P. N.; Bradley, P. M.; Debierre, J.-M. Scaling Behavior of Percolation Surfaces in Three-Dimensions. *Phys. Rev. Lett.* **1991**, *66*, 1330–1333.

(16) Stauffer, D.; Aharony, A. *Introduction to Percolation Theory*; Taylor and Francis: London, 1992.

(17) Gimel, J. C.; Nicolai, T.; Durand, D. 3D Monte Carlo Simulations of Diffusion Limited Cluster Aggregation up to the Sol-Gel Transition: Structure and Kinetics. *J. Sol-Gel Sci. Technol.* **1999**, *15*, 129–136.

(18) Hasmy, A.; Jullien, R. Percolation in Cluster-Cluster Aggregation Processes. *Phys. Rev. E* **1996**, *53*, 1789–1794.

(19) Fry, D.; Chakrabarti, A.; Sorensen, C. M. Manuscript in preparation.

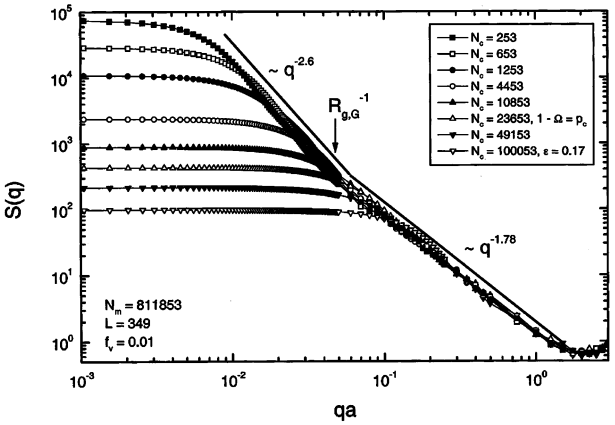

Figure 2. Three-dimensional DLCA simulation results for the structure factor of the *largest* aggregate at various aggregation times for a monomer volume fraction of $f_v = 0.01$. N_m is the number of monomers, L is the box size in units of monomer radius a, N_c is the total number of clusters, which decreases with time, $1 - \Omega$ is the cluster volume fraction, which equals the three-dimensional percolation value $p_C \simeq 0.31$ at the ideal gel point, and $R_{g,G}$ is the ideal gel-point radius of gyration.

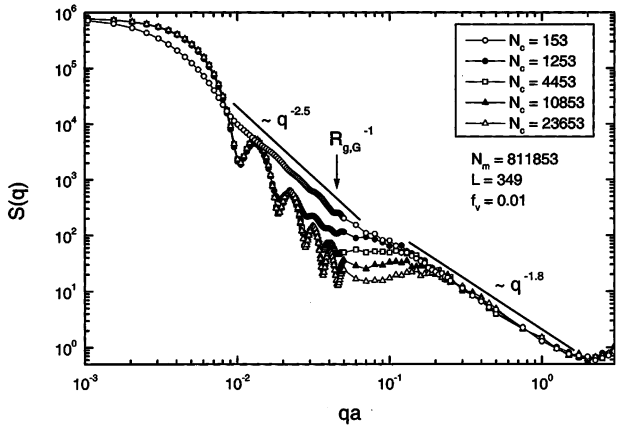

Figure 3. Three-dimensional DLCA simulation results for the structure factor of the *entire* system at various aggregation times for a monomer volume fraction of $f_v = 0.01$. N_m is the number of monomers and L is the box size in units of monomer radius a. N_c is the total number of clusters, which increases with time, and $R_{g,G}$ is the ideal gel-point radius of gyration. The ideal gel point is at $N_c = 23\,653$. Note that for some time after the ideal gel point and $qa < 0.04$, the Porod regime of the box is seen with a characteristic ripple structure. This eventually gives way to $S(q)$ for the superaggregates in the box.

as many as 3×10^6 spherical monomers in a cubic box of side length $L \leq 580$ monomer diameters. Initially, all monomers are treated as clusters of size $N = 1$ with a radius a. The simulation then proceeds by first randomly picking, with probability N_c^{-1}, a cluster of size N, where N_c is the number of clusters at time t. Invoking Stokes–Einstein type diffusion, a cluster is moved, with probability N^{-1/D_0}, one monomer diameter in a randomly chosen direction (i.e., off-lattice), with $D_0 = 1.8$. Each time a cluster is picked, the time, measured in Monte Carlo steps per cluster, is incremented by N_c^{-1} regardless of whether the cluster has moved. If two clusters collide and, hence, aggregate, the motion is adjusted to compensate for any overlap between particles. At various stages of the simulation, the largest cluster and the entire system were Fourier transformed to yield the static structure factor $S(q)$.

Figure 2 shows the structure factor of the *largest cluster* in the system at various times of aggregation for a monomer volume fraction of $f_v = 10^{-2}$. Early in the aggregation, the $S(q)$ characteristic of a $D \simeq 1.8$, DLCA aggregate is seen. With increasing aggregation time, the biggest cluster gets larger, as is indicated by the decreasing value of q at the bend in $S(q)$. This is as was expected. The new result in Figure 2 is that deep in the aggregation, parametrized by comparing the aggregate radius of gyration to the ideal gel-point radius of gyration (see eq 2 to follow), and near the gel point, the structure factor evolves to show two power-law regimes. The $D \simeq 1.8$ regime remains, but at low q and, hence, a large length scale, a $D \simeq 2.6$ regime appears. This second regime grows until the system gels; that is, the largest cluster spans one dimension of the box. The implication of this result is that late in the aggregation near and at the gel point, the largest cluster in the system has a short-range *local* structure described by a fractal dimension of 1.8 and a long-range *overall* structure described by a fractal dimension of 2.6.

The physical significance of this heterogeneous structure becomes clear with the following explanation of the crossover length scale between the $D \simeq 1.8$ and 2.6 regimes in Figure 2. Because the fractal dimension of the aggregates is less than the spatial dimension, when the aggregation proceeds to a certain *critical size*, the aggregates will fill the entire volume, they will touch, and the system will gel. This occurs approximately when the average monomer volume fraction of the clusters equals the overall monomer volume fraction of the system. To calculate the aggregate radius of gyration when this occurs, we idealize the system by assuming that the clusters are monodisperse and spherical. Then the monomer volume fraction in the aggregates is $N(a/R_p)^3$, where N is the number of monomers in the aggregate with a perimeter radius of $R_p = [(D + 2)/D]^{1/2}R_g$.[20] When $N = k_0(R_g/a)^D$, where $k_0 = 1.3$ (ref 21) for DLCA aggregates, is used, the *ideal gel-point radius of gyration* is

$$R_{g,G} = a\{[(D + 2)/D]^{3/2}k_0^{-1}f_v\}^{1/(D-3)} \qquad (2)$$

Because the system is idealized and the boundaries of the aggregates are ill-defined, eq 2 is an approximation.

The inverse of this ideal gel-point radius of gyration is shown as an arrow in Figure 2. This corresponds very well to the crossover wavevector between the $D \simeq 1.8$ and the $D \simeq 2.5$ regimes. A similarly good agreement was found for other volume fractions in the entire range we investigated, $0.1 \geq f_v \geq 5 \times 10^{-4}$. We also remark that the real-space analysis of the largest clusters also show this same morphological crossover at $R_{g,G}$, although not as clearly.[22] Thus, the ideal gel-point radius of gyration is the crossover length scale.

To make a direct comparison to experiment, Figure 3 gives the Fourier transform, hence, the static structure factor, of the *entire* simulated system for $f_v = 10^{-2}$ as a function of time. Late in the aggregation, past the ideal gel point, $S(q)$ shows two regimes. At large q, a slope of -1.8 and, at lower q, a slope of -2.5 result, very similar to the data of Figure 1. We interpret the high q feature as due to both the $D = 1.8$ fractal aggregates of small size and the $D = 1.8$ small-scale part of any superaggregates present. The low q feature is due to the large scale, percolated $D \simeq 2.6$ part of the superaggregates present.

(20) Oh, C.; Sorensen, C. M. The Effect of Monomer Overlap on the Morphology of Fractal Aggregates. *J. Colloid Interface Sci.* **1997**, *193*, 17–25.

(21) Sorensen, C. M.; Roberts, G. C. The Prefactor of Fractal Aggregates. *J. Colloid Interface Sci.* **1997**, *186*, 447–452.

(22) We have found that reciprocal space shows structural crossovers more clearly than real space; see Oh, C.; Sorensen, C. M. Structure Factor of DLA Aggregates. *Phys. Rev. E* **1998**, *57*, 784–790.

The similarity between Figures 3 and 1 implies that Figure 1 gives direct evidence for the DLCA, $D \simeq 1.8$ soot aggregates at low heights (early times) percolating at higher heights in the flame to gel-like $D \simeq 2.6$ percolation superaggregates.

To further substantiate this interpretation, we qualitatively measured the volume fraction of the soot monomers in the flame with light extinction measurements and then calculated $R_{g,G}$ with eq 1. Standard light extinction techniques relying upon absorption-dominating scattering are accurate only for soot clusters smaller than a few tenths of a micrometer.[9] Thus, we measured the extinction of light low in the flame where small aggregates exist and made the reasonable assumption, based on previous diffusion flame measurements,[23] that the total amount of soot volume does not change significantly with the height above burner. Extinction obeys

$$I_T = I_0 e^{-\tau x} \tag{3}$$

where I_T is the light intensity transmitted after passing through a flame of thickness x given an incident intensity I_0. The turbidity is τ, which is related to the soot monomer volume fraction by

$$f_v = \tau/3kE(m) \tag{4}$$

where $E(m) = Im[(m^2 - 1)/(m^2 + 2)]$, where m is the soot refractive index. For m, we use the value $m = 1.56 - i0.56$.[13]

The greatest uncertainty in the determination of f_v involves the path length x. Low in the flame, $h \lesssim 4$ cm, we found intensity ratios of $I_T/I_0 \simeq 0.32$ and $x \simeq 2$ mm. With this, we find $f_v = 6 \times 10^{-5}$ low in the flame. However, at large heights we find that the flame front compresses to yield $x \simeq 100$ μm. This implies $f_v \simeq 10^{-3}$ in the region where the superaggregates form. Use of this rough f_v in eq 2 yields an ideal gel-point radius of gyration of $R_{g,G} \simeq 4$ μm. This is in rough accord with the observed crossover between the $D \simeq 1.8$ and the $D \simeq 2.7$ regimes seen in Figure 1. This nice correspondence between the simulation and the flame results suggests that the $D \simeq 2.6$ soot superaggregates in the flame formed via a process of percolation of smaller, $D \simeq 1.8$ aggregates that formed via the DLCA process earlier in the flame.

2. Restructuring Scenario. Large fractal aggregates formed in colloids have been found to restructure to denser and, hence, larger D, aggregates when subjected to shear. Martin et al.[24] found that colloidal silica aggregates formed via DLCA with a fractal dimension of $D = 1.85$ increased to $D = 1.94$ and 2.12 upon either gently swirling or shaking, respectively, the colloid. In another experiment, large aggregates, which had settled to the bottom of the container and then were resuspended, showed a structure factor with a crossover in slope from -1.7, at large q, to -2.5, at small q. Martin et al. suggested that the shear stresses involved in the resuspension restructured the aggregates to create the $D \simeq 2.5$ regime. This crossover is very similar to that seen in Figure 3, which implies a percolation scenario. However, our calculation of $R_{g,G}$ for their system does not correspond to this crossover; hence, percolation is not supported. This leaves restructuring.

Carpineti et al.[25] saw similar shear-induced changes in polystyrene colloids that had been destabilized to form $D \simeq 1.8$ fractal aggregates. They found that stronger shears gave more pronounced effects and, in one case, saw a structure factor similar to that in Figure 3.

More recently, Jung et al.[26] formed iron hydroxide flocs while vigorously stirring. Thus, monomers grew to aggregates with the continuous presence of shear. The result was aggregates with fractal dimensions of $D = 2.52-2.71$, the larger values corresponding to larger shear rates. These D values were measured in the size range (inverse q) of about 0.8−120 μm, as was allowed for by their small-angle light scattering apparatus.

There is certainly an unmistakable sameness in our observed fractal dimension for our soot superaggregates with $D \simeq 2.6$ and these cases of heavily sheared colloidal aggregates, also with $D \simeq 2.6$. We can estimate that shear on the order of 100 sec^{-1} exists along the flame front. There is also some yet to be described mechanism that compresses the flame front thickness by about 1 order of magnitude. Thus, shear is strongly implicated as the cause of the superaggregates. However, without a model of how shear restructures DLCA aggregates and a quantitative measure of the shear field in the flame, a definitive assignment cannot be made.

V. Conclusion

We have found that supersoot aggregates that appear in acetylene/air laminar diffusion flames have a fractal dimension of $D \simeq 2.6$ over the length scales of about 1−10 μm and a fractal dimension of $D \simeq 1.8$ over length scales from (presumably) the monomer (or primary particle) length scale of about 30 nm up to 1 μm. The mechanism by which these superaggregates form the $D \simeq 2.6$ structure is unknown but likely due either to percolation of submicrometer $D \simeq 1.8$ aggregates or to the restructuring of these aggregates due to shear (or, perhaps, some other force) as they grow into the supramicrometer range. Finally, the mechanism by which these superaggregates come together to form the two-dimensional soot at the 100 μm scale[8] also remains to be understood.

Acknowledgment. This work was supported by NASA Grant NAG 3-2360 and NSF Grant CTS0080017.

LA034063H

(23) Santoro, R. J.; Semerjian, H. G.; Dobbins, R. A. Soot Particle Measurements in Diffusion Flames. *Combust. Flame* **1983**, *51*, 203−223.

(24) Martin, J. E.; Wilcoxon, J. P.; Schaefer, D.; Odinek, J. Fast Aggregation of Colloidal Silica. *Phys. Rev. A* **1990**, *41*, 4379−4391.

(25) Carpineti, M.; Ferri, F.; Giglio, M.; Paganini, E.; Perini, U. Salt-Induced Fast Aggregation of Polystyrene Latex. *Phys. Rev. A* **1990**, *42*, 7347−7354.

(26) Jung, S. J.; Amal, R.; Raper, J. A. Monitoring Effects of Shearing on Floe Structure Using Small-Angle Light Scattering. *Powder Technol.* **1996**, *88*, 51−54.